Copyright © 2018 by The Journal of Bone and Joint Surgery, Incorporated

Retrieval Findings of Recalled Dual-Taper Hips

Anna Di Laura, MSc, Harry S. Hothi, PhD, Johann Henckel, MD, Young-Min Kwon, MD, PhD, John A. Skinner, FRCS(Orth), and Alister J. Hart, FRCSG(Orth)

Investigation performed at the Institute of Orthopaedics and Musculoskeletal Science, University College London and the Royal National Orthopaedic Hospital, Stanmore, United Kingdom

Background: The recent high-profile recalls of several dual-taper hip designs pose questions regarding why those designs perform poorly. We aimed to characterize taper damage in 1 recalled design to understand failure mechanisms to inform surgeons on which patients should be considered at risk of revision and when to revise.

Methods: High-precision measurement equipment was used to characterize the metal loss from the neck-stem interface of 116 retrieved Rejuvenate femoral stems (Stryker Howmedica Osteonics) revised because of an adverse reaction to metal debris. Head-neck taper surfaces were also investigated, and clinical and laboratory data were examined.

Results: The neck-stem junction of each implant was moderately to severely corroded and showed a characteristic wear pattern on both male and female taper surfaces. The severity of taper damage was positively correlated with time to revision (coefficient, 0.040 [95% confidence interval (CI), 0.028 to 0.051]; $p < 0.0001$) and with serum cobalt concentration (coefficient, 0.02 [95% CI, 0.01 to 0.02]; $p < 0.0001$) and serum chromium concentration (coefficient, 0.04 [95% CI, 0.009 to 0.070]; $p = 0.0142$).

Conclusions: A forensic examination of the retrieved components that failed secondary to an adverse reaction to metal debris showed, in all cases, visible corrosion. Of the implant and patient factors investigated, we did not identify any predictors of corrosion. The severity of damage was found to increase with time; cobalt was significantly elevated over chromium.

Clinical Relevance: Surgeons should scrupulously follow and consider revision for patients with this implant design to avoid extensive tissue excision. Blood metal ion tests may aid in identifying the mechanisms of taper corrosion.

Dual-taper hip implants offer surgeons a more flexible solution to match the patient's anatomy and to provide a more personalized form of joint replacement. However, the extra taper junction between the neck and the stem increases the risk of clinical failure twofold compared with fixed stems, and, within the dual-taper-design population, the titanium and cobalt-chromium metal combination has a higher rate of revision compared with the titanium and titanium type[1].

Concerns related to neck-stem junctions embrace a variety of complications from neck fracture[2-5] to corrosion[6-15] and subsequent metal-related reactions[6,8,16-20] from cold welding[21] to disassociation[22,23]. Recently, attention has been brought to a specific design (Rejuvenate; Stryker Howmedica Osteonics) recalled in 2012 by the manufacturer because of high revision rates as a result of metal debris from the modular stem junction. At the time of the recall, >30,000 patients had received this design of a modular stem worldwide.

For the Rejuvenate design, survivorships of 69.3% at 2 years[24] and of 40% at 4 years[6] have been reported. It has been shown that tribocorrosion is the predominant mechanism for metal release from the conical-shaped aspects of the neck male tapers and that the time to revision plays a role in the progression of taper damage[25]. Taper design[26] and material combination[27] have been identified as potential factors in neck-stem taper corrosion. However, the clinical symptoms related to the failure of this design are not fully understood.

The purpose of this study was to identify risk factors for taper damage in the Rejuvenate dual-taper hip replacements, so as to help surgeons to understand who should be considered at risk of revision. Neck-stem junctions were assessed for the severity of fretting-corrosion damage and the amount and location of material lost; and the link between our findings and clinical variables, using a multivariate linear regression model, was investigated.

Disclosure: Two authors of this study (J.A.S. and A.J.H.) received a grant from Stryker; the funds were used to pay for the retrieval analysis. The **Disclosure of Potential Conflicts of Interest** forms are provided with the online version of the article (http://links.lww.com/JBJS/E914).

Materials and Methods

Retrieved Explants

This study was designed as a descriptive retrospective case series involving all of the 116 retrieved dual-taper Rejuvenate design hip implants sent to our center for analysis. The body of the Rejuvenate stem design is made of a Stryker-patented beta titanium-based alloy (Ti-12Mo-6Zr-2Fe, or TMZF). The neck is made of a wrought cobalt-chromium-molybdenum alloy. The bearing surfaces in the cohort examined consisted of cobalt-chromium-molybdenum (LFIT [low friction ion treatment] cobalt-chromium [CoCr]; Stryker) or ceramic (BIOLOX delta; CeramTec) femoral heads articulating with ultrahigh molecular weight acetabular liners (in the standard fixed cup configuration [n = 64]) or highly cross-linked polyethylene liners (in the dual-mobility configuration [n = 52]).

Patient Demographic Characteristics

Preoperative data concerning the revised arthroplasties were collected. Components were explanted from 63 male patients and 53 female patients with a median age of 64 years (range, 36 to 92 years) and a median body mass index (BMI) of 29.1 kg/m^2 (range, 20 to 46.7 kg/m^2). The median time from implantation was 34 months (range, 12 to 71 months). Blood serum cobalt and chromium levels that were recorded prior to revision were available for approximately 80% of the cases, and cobalt levels were significantly higher than chromium levels in the blood (t test, $p < 0.0001$) (Table I).

The patients underwent revision surgical procedures as a result of adverse local tissue reactions resulting in pain, elevated metal ion levels, and fluid collection or masses revealed by magnetic resonance imaging. The study was approved by our institutional review board; all patients gave informed consent for nondestructive analysis of the prosthesis.

TABLE I Patient Demographic Characteristics, Implant Details, and Metal Ion Concentrations*

Variable	Value
Sex*	
Male	63
Female	53
Age at primary surgery† *(yr)*	64 (36 to 92)
Time to revision† *(mo)*	34 (12 to 71)
BMI† *(kg/m²)*	29.1 (20 to 46.7)
Bearing type*	
Dual-mobility	52
Standard	64
Material of the head*	
Ceramic	74
Metal	42
Neck length† *(mm)*	34 (30 to 42)
Total implant offset† *(mm)*	44 (34.9 to 53.9)
Blood serum metal ion levels† *(µg/L)*	
Cobalt	7.4 (0.3 to 34)
Chromium	1.7 (0.1 to 14)
Cobalt/chromium ratio	4.5 (0.16 to 13.6)

*The values are given as the number of patients. †The values are given as the median, with the range in parentheses.

Neck-Stem Junction

Qualitative Assessment of Taper Damage

Each stem and neck taper was visually examined by 2 observers and was graded according to the scoring system of Goldberg et al.[28] for signs of corrosion apparent under stereomicroscopy (VHX-700F series; Keyence): none indicates grade 1, mild indicates grade 2, moderate indicates grade 3, and severe indicates grade 4. Both the external neck taper and internal stem taper surfaces, hereafter referred to in this study as the neck male and the female stem taper surface, were divided into 4 zones, corresponding to the flat surfaces (anterior, posterior) and conical surfaces (medial, lateral) (Fig. 1); the mean value of the 4 zones gave the overall Goldberg score.

Three-Dimensional Mapping for Distribution of Taper Damage

The initial characterization of taper damage was achieved by selecting a consecutive series of components to perform 3-dimensional mapping of the conical aspects of the neck and internally in the stem bore tapers to record the location of the damage and eventual wear patterns.

To obtain this, we used a Talyrond 365 contacting profilometer roundness-measuring machine (Taylor Hobson) to quantify the material lost from the head-neck taper junctions. The 360 traces, spaced at 0.5° intervals to each other, were taken on the conical-shaped aspects to detect and display very fine details of the metal topography.

We focused on the examination of the conical-shaped aspects of the neck male tapers, which constitute three-fourths of the whole taper, excluding the flat sides, as they have been shown to be the area in which the damage is predominantly localized[13,25,27].

Scanning Electron Microscopy and Elemental Analysis

A subset of the necks that showed macroscopic and microscopic signs of severe corrosive damage was further analyzed using scanning electron microscopy (HITACHI S-3400 N; Hitachi) equipped with energy-dispersive x-ray spectroscopy (EDS) for surface and compositional characterization.

Quantitative Assessment of Taper Damage

Based on the observation of consistent patterns of localized taper damage and its distribution on the surface of the neck male tapers, a measurement method, using the Talyrond 365 contacting profilometer roundness-measuring machine, was adopted to quantify damage severity on the conical-shaped segments of the male tapers. Ten longitudinal traces taken along the taper axis were individually normalized

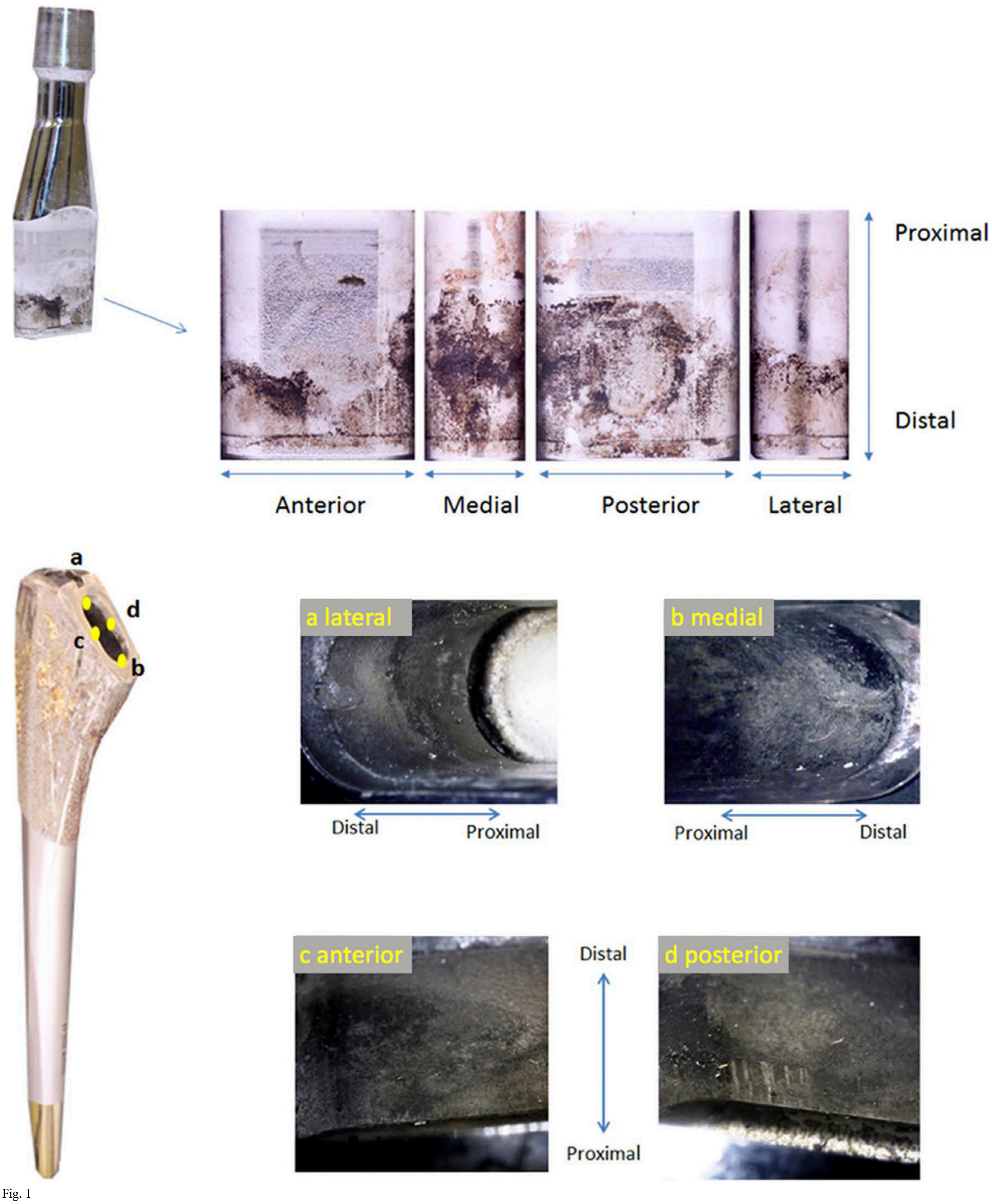

Fig. 1

A panoramic view composed of photographs of the 2 flat and 2 conical surfaces of the neck (upper image) and stem tapers (bottom image). These were graded for severity of corrosion using a scale from 1 to 4 (from no visible corrosion to >10% of the surface containing black debris, pits, or etch marks).

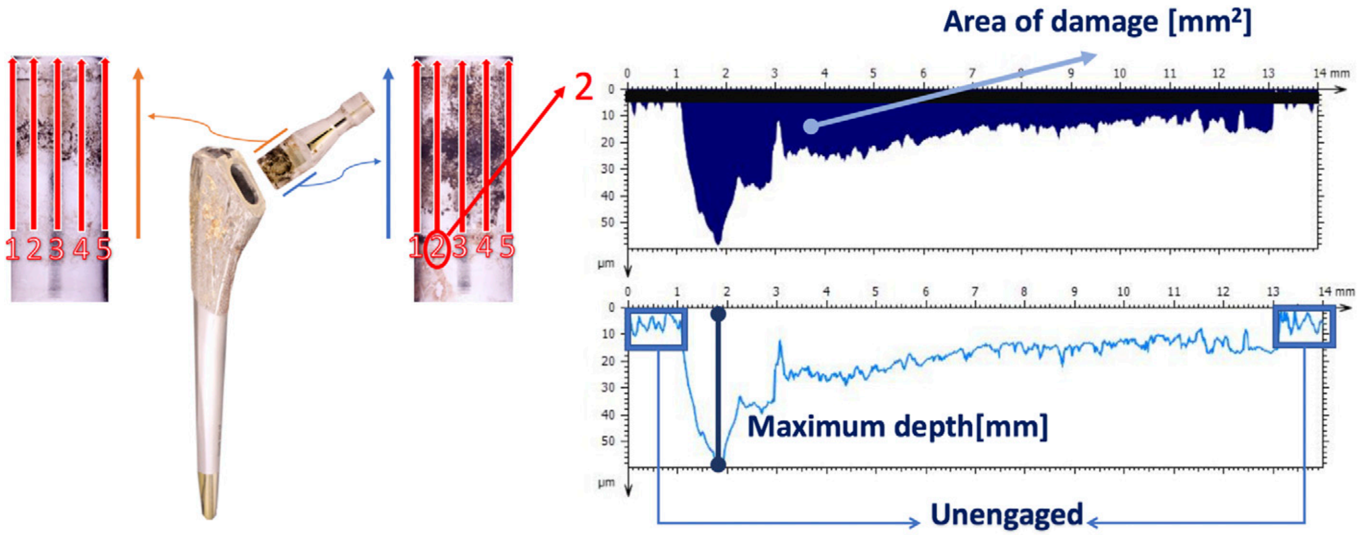

Fig. 2

Illustrative schematic of the methods. Ten longitudinal traces were taken at 45° increments on the conical segments of the neck male tapers, they were normalized relative to an unaffected (unengaged) surface, and a wear area for the trace was calculated. The summed area of these 5 traces provided a measure of surface damage for comparative purposes. Maximum linear wear depth was also recorded.

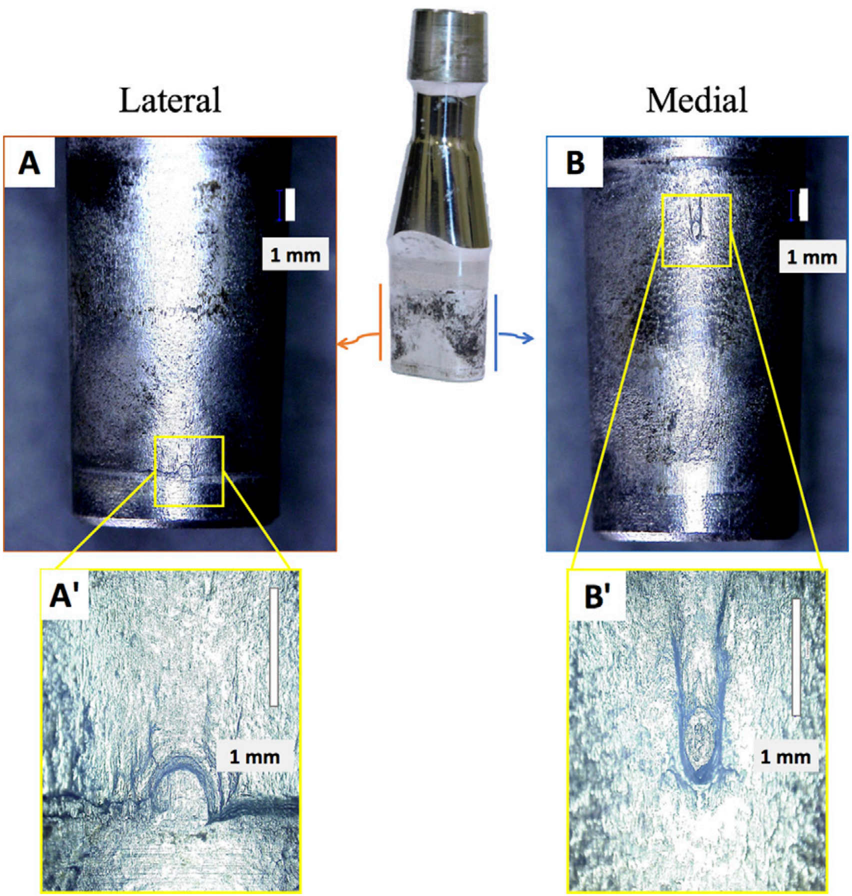

Fig. 3

Microscopy of the neck surfaces. **Fig. 3-A** Lateral side showing a dome-shaped feature approximately one-half millimeter in length surrounded by wear and corrosion damage; striations indicative of plastic deformation and shear were present all around the patch (bottom figure). **Fig. 3-B** Medial side showing an oblong-shaped feature corresponding with the major contact stress region within the stem (magnification, ×30 and ×100).

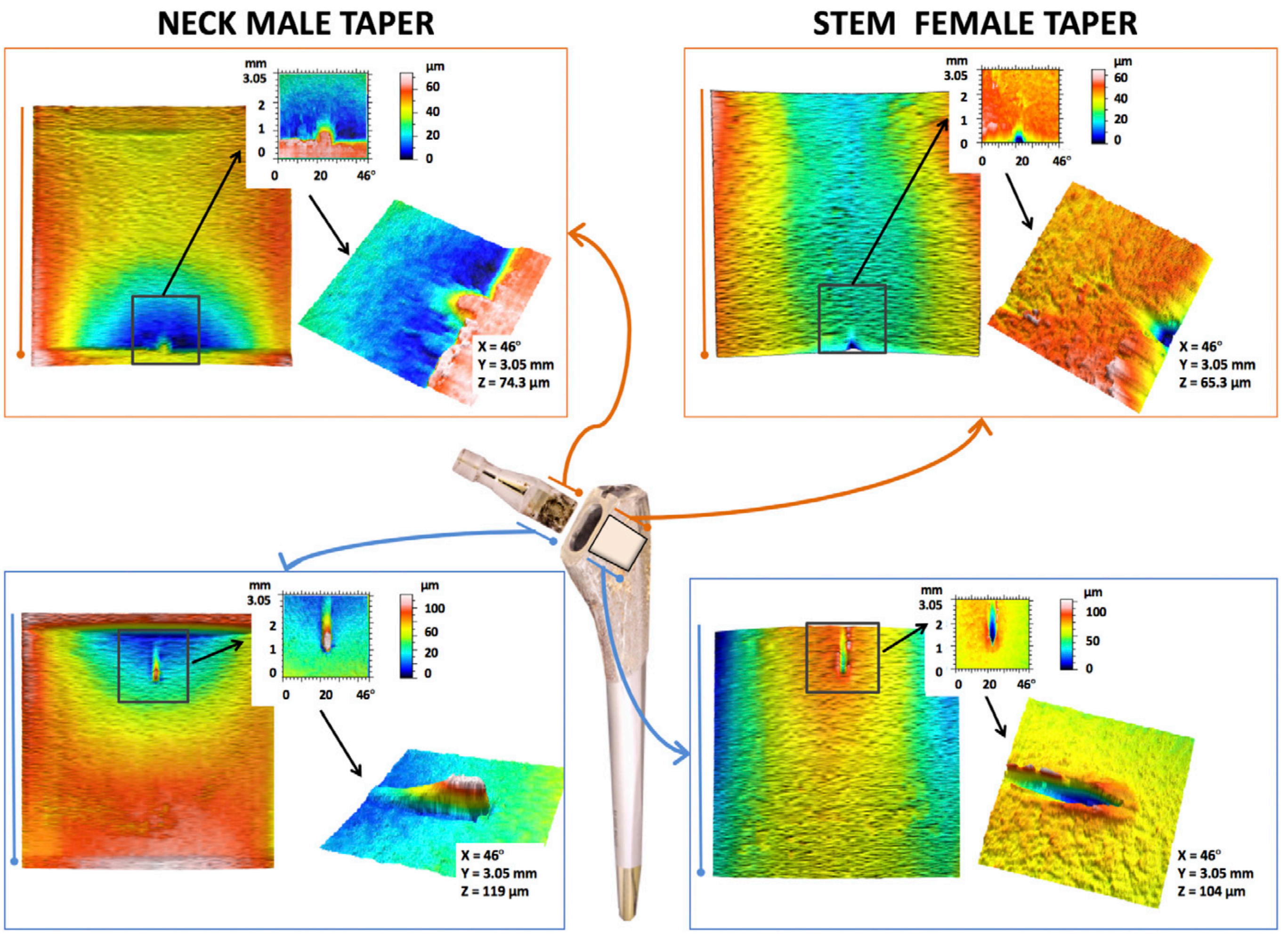

Fig. 4

Three-dimensional color maps of the lateral and medial conical aspects of the neck male tapers (left) and the stem female tapers (right) showing the deepest areas of surface damage in blue compared with the as-manufactured surface in red. The square maps represent the opening of the conical-shaped regions scanned with the surface profilometer; wear depth is expressed in microns. The cobalt-chromium tapers presented patches (positive features, red) with preserved topography with material loss all around them (blue areas) on the neck male tapers (left). The TMZF tapers presented no specific localization of metal lost compared with the cobalt-chromium necks (right). Complementary patches, equal in size and shape (negative features) to those reported on the necks, were seen but with no localized metal loss around them.

relative to the unengaged, and thus unaffected, surface of the taper. The sectional area of the damage was calculated in square millimeters, and the maximum linear penetration depth was recorded (Fig. 2). The maximum linear penetration depths on both medial and lateral aspects of the necks were strongly correlated with the summed areas of the traces (see Appendix). Therefore, the summed area of these 10 traces per neck provided a measure of surface damage for a comparative purpose within our cohort. The details of the method are reported in the Appendix.

Head-Neck Junction

Quantitative Assessment of Taper Damage

The volume of material loss from the head-neck junction of a subset of 48 implants was measured and was analyzed using the Talyrond 365 roundness-measuring machine[29]. The subset was a consecutive series of ceramic and metal heads with standard fixed polyethylene bearing type so as to account for both material combinations[30]. The median values of the scores for corrosion damage (Goldberg score) were significantly lower at both the head bore surface ($p = 0.0006$) and the trunnion taper surface ($p = 0.0009$) in the implants featuring a dual-mobility type of bearing.

Statistical Methods

Descriptive statistics were used to examine surgical, implant, and patient-related factors investigated in association with the outcome of interest, the summed area in square millimeters of the 10 two-dimensional traces taken along the neck male tapers. The variables investigated were sex, age at the time of the primary surgical procedure, BMI, time to revision, head diameter, implant horizontal offset, neck length, and outer

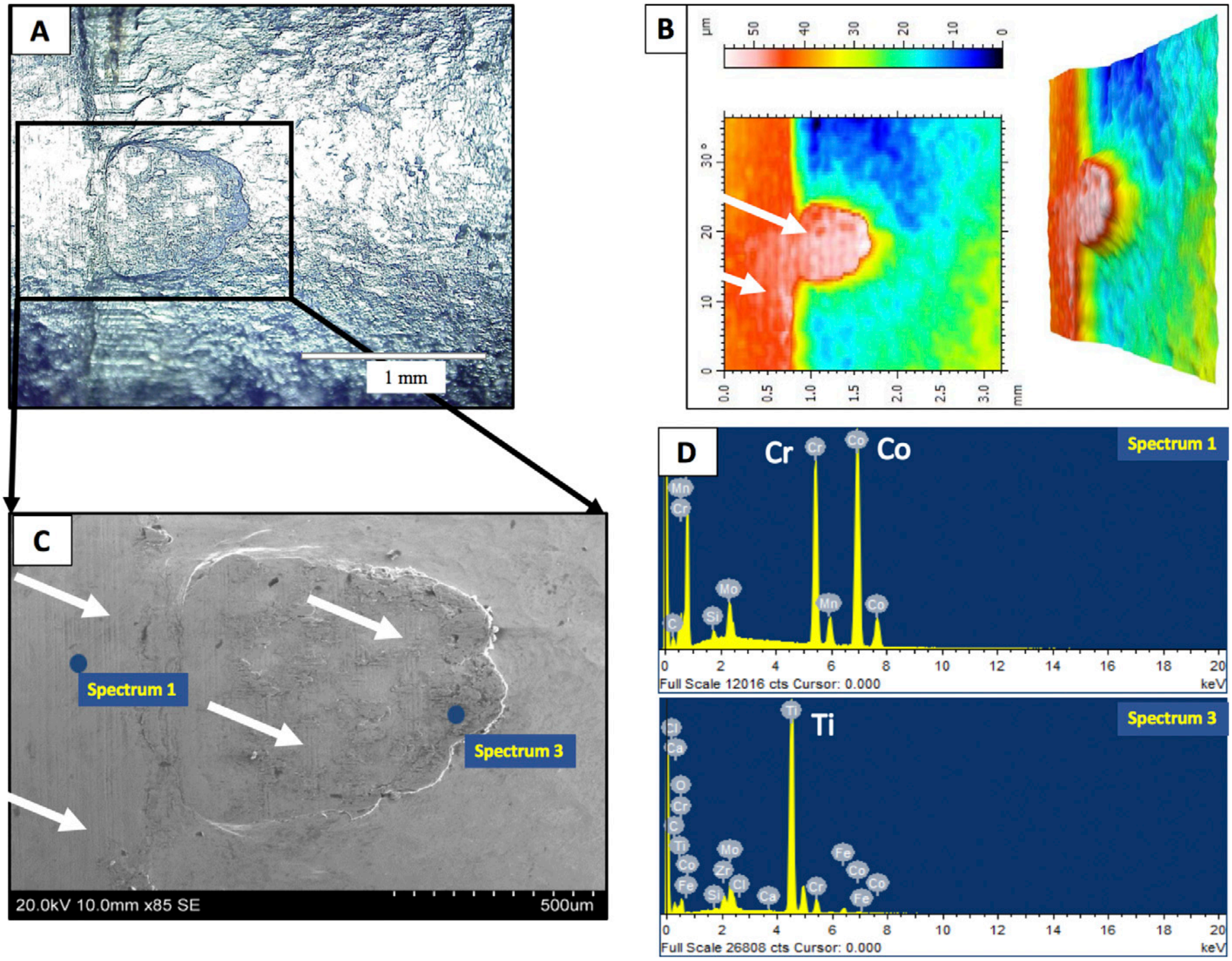

Fig. 5

Fig. 5-A Digital optical micrograph of a neck highlighting a characteristic patch (black box) on the lateral aspect of the taper surface. **Figs. 5-B and 5-C** Surface profilometry of the same patch (**Fig. 5-B**) and electron microscope image (**Fig. 5-C**) of the region, both showing a retained topography, identified by unidirectional machining lines (white arrows) visible on the unengaged part of the necks. **Fig. 5-D** EDS spectra showing TMZF alloy transfer corresponding with the retained surface texture.

diameter of the polyethylene liner in the case of dual-mobility cups.

The association was first assessed using univariate linear regression models. Linear regression was also used to perform univariate analysis of the relationship of the cobalt and chromium variables with the rate of damage (mm^2/yr). A multivariate linear regression model was then fitted, selecting those risk factors that were significant at $p < 0.05$ using a backward selection model.

The implants were analyzed using independent t tests according to their bearing type (dual-mobility and standard bearing) and, within these 2 groups, by the material of the head (ceramic and metal). Independent t tests were also used to explore the difference in maximum wear depth between the medial and lateral aspects of the necks. The intraclass correlation coefficient (ICC) was used to test the reproducibility of the method of analysis performed by the 2 examiners.

Results

Neck-Stem Junction

Qualitative Assessment of Taper Damage

The neck-stem taper junctions showed severe corrosion in the majority of cases, with a median score of 4 and range from 3 to 4 for both neck and stem taper surfaces. Extensive black areas, discoloration, and changes in surface roughness were common features observed in our cohort (Fig. 1). A peculiarity was observed both visually and microscopically; the necks presented oblong-shaped patterns on the medial proximal sides and dome-shaped patterns on the lateral distal sides corresponding with regions of major stresses (Fig. 3).

The Journal of Bone & Joint Surgery · jbjs.org
Volume 100-A · Number 19 · October 3, 2018

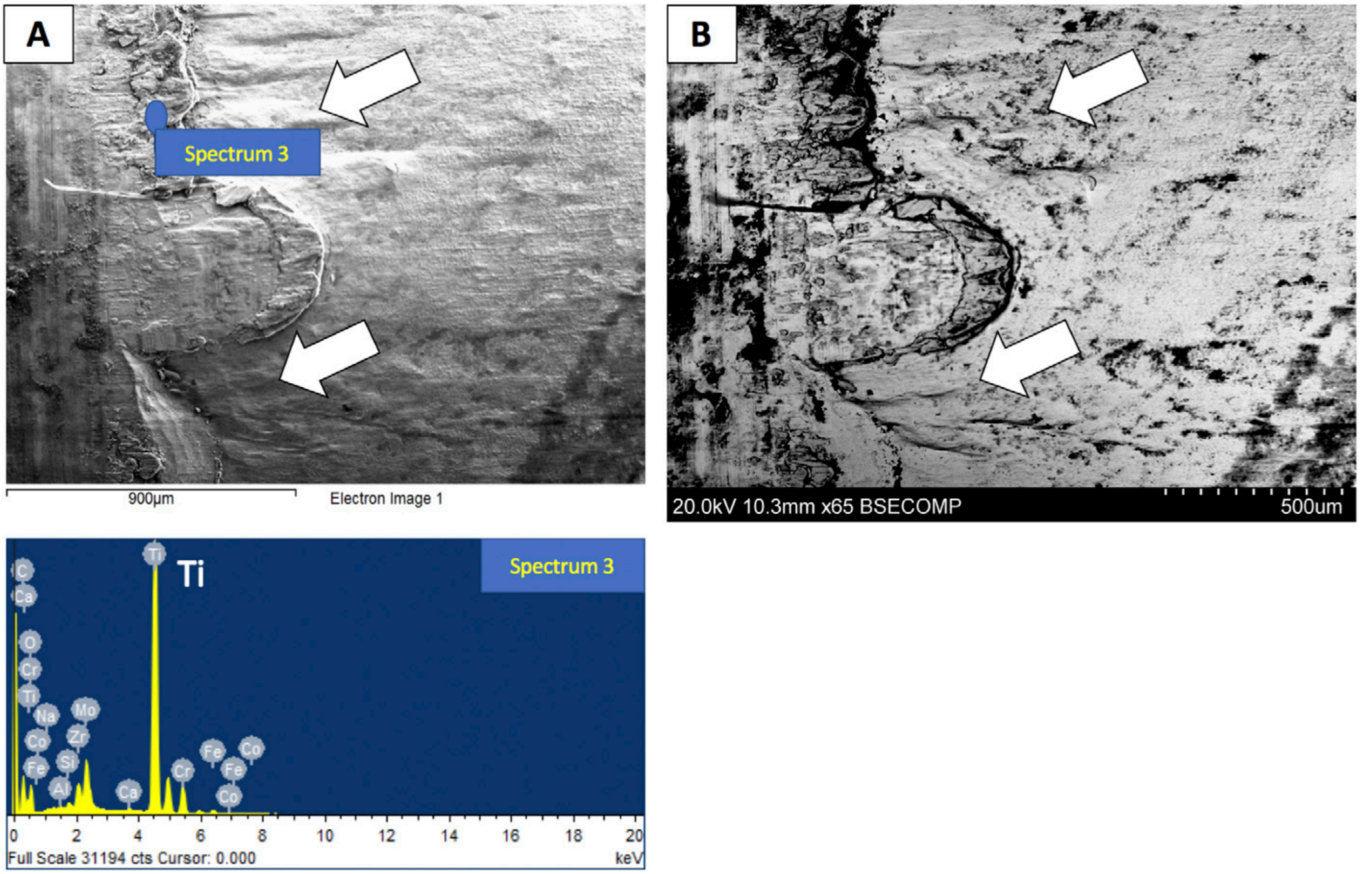

Fig. 6

Scanning electron micrographs and an EDS spectrum of the cobalt-chromium alloy neck presented in Figure 3 (lateral side). Unidirectional wavelike topography (white arrows), indicating sliding and plastic deformation, were seen with both the secondary electron modality (**Fig. 6-A**) and the backscattered electron modality (**Fig. 6-B**).

Three-Dimensional Mapping for Distribution of Taper Damage

This procedure allowed the observation and further characterization of the peculiar pattern of wear damage on the necks involving oblong-shaped patterns on the medial sides and dome-shaped patterns on the lateral sides, corresponding with regions of high stresses, with depletion of metal all around these patches. Three-dimensional maps showed a corresponding complementary wear pattern at the stem bore taper, and the size and shape of the positive features on the necks were complementary to those on the stem tapers, a coup-countercoup pattern compatible with cantilever bending. However, conversely to what was seen on the male components, the damage was not extensive and/or localized around the patches compared with the necks (Fig. 4).

Scanning Electron Microscopy and Elemental Analysis

Chromium-rich deposits were found composing the black debris. Traces of titanium, zirconium, and iron were also present as a consequence of metal transfer from the stem to the neck. Titanium-rich spectra contained elevated oxygen content indicating an oxide form.

A layer of titanium was found covering points of major stresses on the neck male parts, in which the initial topography was maintained while the surface all around those patterns exhibited worn (Fig. 5), unidirectional wavelike topography, indicating sliding and plastic deformation[31] (Fig. 6).

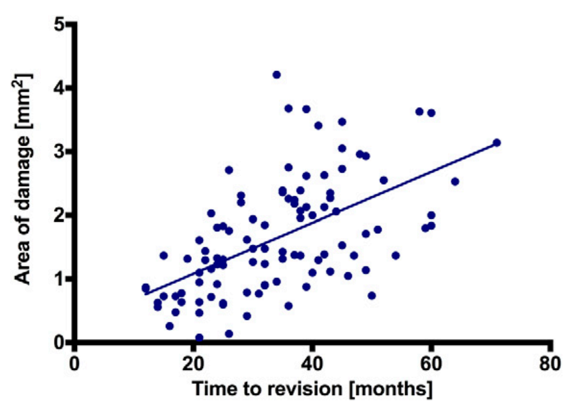

Fig. 7

XY scatterplot showing severity of damage compared with time to revision. Findings showed that, for every 1-unit increase in time, there was a 0.04-unit increase in the summed area of the 10 traces taken along the taper (median, 0.040 [95% CI, 0.03 to 0.05]; $p < 0.0001$).

Quantitative Assessment of Taper Damage

The univariate linear regression models showed significant and positive associations between the summed area of the 10 traces taken along the neck male taper and time to revision (coefficient, 0.040 [95% confidence interval (CI), 0.028 to 0.051]; $p < 0.0001$) (Fig. 7). For every 1-unit increase in time, there was a 0.04-unit increase in the sum of the 10 traces taken along the taper.

No significant relationship was detected between the summed area of the 10 traces and any of the following variables: age, sex, BMI, head diameter, implant horizontal offset, neck length, and outer diameter of polyethylene liners of dual-mobility cups (Table II). There was no significant difference in area of damage between bearing group types (dual-mobility or standard) or head materials (ceramic and/or metal) (t test, $p > 0.05$).

Reproducibility

The ICC showed excellent reproducibility between the 2 examiners for the measurement of the area of damage (ICC, 0.95 [95% CI, 0.87 to 0.98]; $p < 0.0001$).

The multivariate analysis showed an association between the severity of taper damage and time to revision ($p < 0.0001$).

There was a positive linear correlation between wear rate (mm^2/yr) and levels in the blood of cobalt (coefficient, 0.02 [95% CI, 0.01 to 0.02]; $p < 0.0001$) and chromium (coefficient, 0.04 [95% CI, 0.009 to 0.07]; $p = 0.0142$) (Fig. 8).

The medial parts of the necks exhibited deeper depth of wear compared with their lateral counterparts (Fig. 9). The maximum linear wear depth on the proximal medial aspect of the necks ranged from 20 to 200 μm, with a mean of 68.25 μm.

TABLE II Univariate Analysis (Linear Regression) Models for Summed Area of the 10 Traces Taken Along the Neck Male Tapers (N = 116)

Variable Compared with Summed Area	Coefficient*	P Value
Female sex	0.234 (−0.100 to 0.568)	0.17
Age in years	−0.0002 (−0.0154 to 0.0151)	0.98
BMI in kg/m²	−0.010 (−0.044 to 0.024)	0.56
Time to revision in months	0.040 (0.028 to 0.051)	<0.0001
Head diameter in mm	−0.009 (−0.044 to 0.027)	0.63
Implant horizontal offset in mm	0.014 (−0.034 to 0.063)	0.55
Neck length in mm	0.006 (−0.037 to 0.050)	0.77
Outer polyethylene diameter in mm	−0.007 (−0.036 to 0.022)	0.65

*The values are given as the coefficient, with the 95% CI in parentheses; this can be interpreted as the increase in the summed area in mm² for a 1-unit increase in the risk factor of interest.

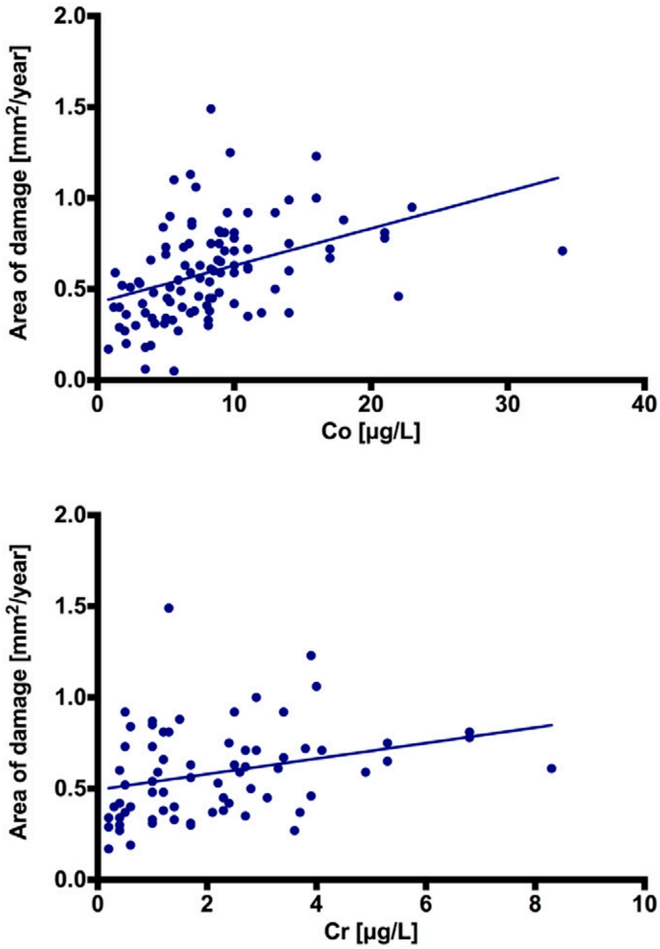

Fig. 8

XY scatterplots showing the relationship between the severity of taper damage (mm^2/yr) and the corresponding cobalt (Co) (upper graph) and chromium (Cr) (bottom graph) concentrations in the blood.

On the lateral side, the mean maximum wear depth was 41.03 μm (range, 8 to 130 μm). The difference between the medial and lateral aspects was found to be significant (t test, $p < 0.0001$).

Head-Neck Junction: Quantitative Assessment of Taper Damage

The median taper material loss rates (both head bore and trunnion surfaces) were 0.210 mm^3/yr (range, 0.030 to 0.448 mm^3/yr) for the metal head group and 0.084 mm^3/yr (range, 0.059 to 0.108 mm^3/yr) for the ceramic head group. The difference was not significant ($p = 0.58$). In all cases, the losses were very low, <1 mm^3/yr[30].

Discussion

We aimed to better understand the impact of clinical and implant factors on the variability of the in vivo performance of recalled dual-taper implants to help surgeons to identify patients at risk of a revision surgical procedure. The analyzed devices were explanted because of an adverse reaction

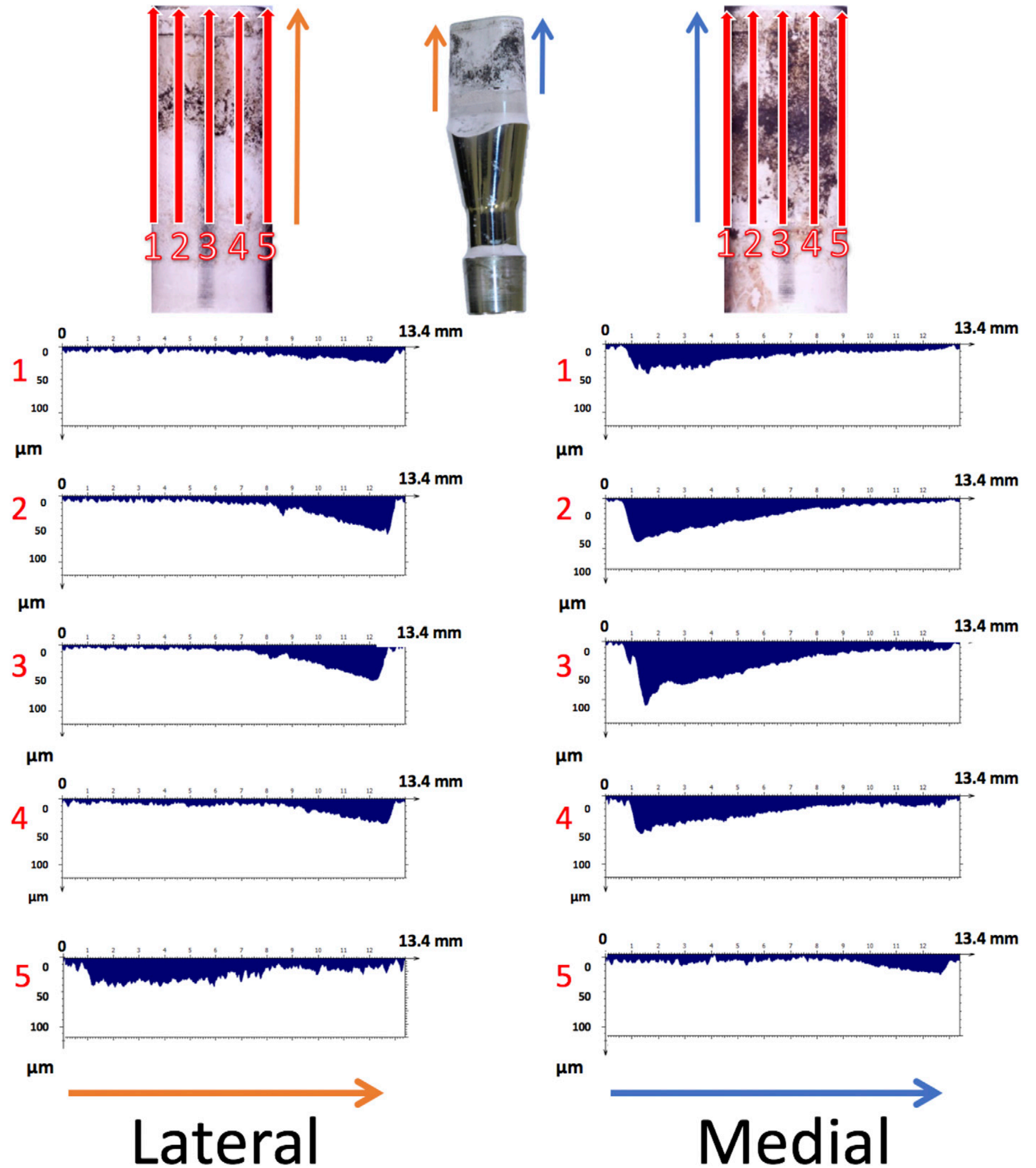

Fig. 9
Example showing the 10 traces taken from the neck of an implant to calculate the relative area of damage and the maximum wear depth. The medial aspect showed the greatest material lost, with the deepest valleys ranging from a few micrometers (trace 5) to >100 µm (trace 3).

to metal debris and had been sent to our center for forensic examination together with the patient's clinical data. We applied engineering methods to evaluate and quantify taper damage and correlated this with the available clinical data. Multivariate analysis using 8 variables from 116 components revealed a strongly significant correlation between neck-stem taper wear and time to revision. Moreover, univariate linear regression analysis showed that the wear rate was significantly associated with increased cobalt and chromium concentrations in the blood.

None of the available implant or patient-specific data correlated with the measured value of material loss observed. The bearing type and material of the heads made no difference in the outcomes measured. The ranges of maximum linear wear depth found were twofold higher than those previously reported for studies looking at head-neck taper junctions with metal-on-metal bearings (cobalt-chromium and titanium combination) that had failed because of an adverse reaction to metal debris[32].

To our knowledge, this current study constitutes the largest retrieval study investigating neck-stem taper damage in dual-taper hip implants. An elevated blood ion ratio of cobalt relative to chromium has been associated with taper damage[33,34], and the present findings support this. Despite their unsatisfactory clinical performance, dual-taper hip implants provide information helpful for understanding the clinical importance of taper corrosion, because there are no confounding effects from metal-on-metal bearings and negligible corrosion or material loss has been reported at the head-neck taper junction[25,30,35].

For the first time for this specific design of implant, the cobalt and chromium concentrations in patients (in other words, the in vivo biomarkers of the wear rate) were available, thus giving a clinical importance to the retrieval analysis. Patients reported significantly elevated median levels of cobalt (7.4 μg/L) and chromium (1.7 μg/L).

Gross evidence of black deposits on all surfaces of the neck-stem taper junctions was found, more extensively on the medial conical aspect (Fig. 1). A number of studies have documented substantial corrosion on the removed components[6,11,13,24,36-40] of this design. Compositional analysis confirmed chromium-rich deposits, phosphorus, and depletion of cobalt, indicative of corrosion processes taking place.

A characteristic wear pattern was observed in areas of maximum stresses. In many cases, the patches showed a retained topography of the original manufactured metal surface with a superficial TMZF transfer (Figs. 4 and 5). These findings are in agreement with recent research[25,27]. In addition, in this current study, the small size of the probe of the contact profilometer allowed us to capture complementary patches on the surfaces of the female taper, the localized removal of the TMZF alloy that had been transferred from the surfaces of the female taper of the stem onto the surface of the necks. The patches were complementary in size and shape to those seen on the surfaces of the neck male tapers (Fig. 4). It appears that, during in vivo function, the high stresses transmitted to the taper junction have led to material transfer of the titanium alloy on the cobalt-chromium alloy in areas of zero or partial slip fretting regime[27]. Although there were extensive areas of metal removal all around the patches on the neck male parts, this was not seen on the female counterparts. This could be partially explained by the increase in interfacial hardness of the TMZF alloy when coupled with the cobalt-chromium alloy[27]. Distribution of taper damage was random and more superficial on the surfaces of the female stem tapers, confirming the process of the hardening of the titanium alloy.

These findings can contribute to the understanding of the complex TMZF and cobalt-chromium interaction in the in vivo environment, considering the recent reports on the gross failure of TMZF trunnions mating with cobalt-chromium heads[41-43].

The recall of this prosthesis, in addition to the disappointing performance of other dual-taper designs, whose approval had been based on the principle of substantial equivalence, once again highlights the importance of long-term clinical trials.

There were limitations in our study. In this cohort of failed implants, none of the patient or implant variables investigated was found to be predictive of failure. This may be because the retrieval analysis could not account for factors that could have had an influence on the severity of taper damage, such as patient activity levels[44] and weight[45] or surgical factors such as taper assembly condition[46] and assembly force[47]. Our findings, although reproducible, cannot be used to directly compare volumetric metal losses; however, we reported maximum wear depths that constitute valuable data for comparison in future work. Moreover, our analysis was restricted by the limitations of the measurement tool, which could only analyze conical-shaped surfaces, thus excluding the contribution of the flat surfaces that account for one-fourth of the whole male tapers.

In conclusion, forensic examination of the retrieved components that failed secondary to adverse reaction to metal debris showed, in all cases, visible corrosion. Maximum linear wear depth recorded was twofold higher than that reported for head bore tapers in cobalt-chromium and titanium couples that failed because of an adverse reaction to metal debris[32]. The severity of damage was found to increase with time in situ and to be associated with an increase of cobalt and chromium concentrations in the blood, thus increasing the risk of adverse tissue reactions. There is evidence in the literature that an increase in the level of cobalt relative to chromium can represent as a biomarker for taper tribocorrosion[8,33,34]. Surgeons should scrupulously follow up and consider revision for these patients to avoid extensive tissue excision.

Appendix

eA A description of the method of measurement of material loss profile and figures showing the correlation of the maximum linear penetration depth on the medial and lateral aspects of the necks with the summed area of the 5 traces are available with the online version of this article as a data supplement at jbjs.org (http://links.lww.com/JBJS/E915). ■

Anna Di Laura, MSc[1]
Harry S. Hothi, PhD[1]
Johann Henckel, MD[1]
Young-Min Kwon, MD, PhD[2]
John A. Skinner, FRCS(Orth)[1]
Alister J. Hart, FRCSG(Orth)[1]

[1]Institute of Orthopaedics and Musculoskeletal Science, University College London and the Royal National Orthopaedic Hospital, Stanmore, United Kingdom

[2]Massachusetts General Hospital, Harvard Medical School, Boston, Massachusetts

E-mail address for A. Di Laura: anna.laura.14@ucl.ac.uk

ORCID iD for A. Di Laura: 0000-0002-4212-3741
ORCID iD for H.S. Hothi: 0000-0001-8745-2111
ORCID iD for J. Henckel: 0000-0003-4086-1609
ORCID iD for J.A. Skinner: 0000-0002-1901-9057
ORCID iD for A.J. Hart: 0000-0003-1281-6886

References

1. The Australian Orthopaedic Association National Joint Replacement Registry. Annual report. Adelaide: AOA; 2015.
2. Dangles CJ, Altstetter CJ. Failure of the modular neck in a total hip arthroplasty. J Arthroplasty. 2010 Oct;25(7):1169.e5-7. Epub 2009 Oct 17.
3. Ellman MB, Levine BR. Fracture of the modular femoral neck component in total hip arthroplasty. J Arthroplasty. 2013 Jan;28(1):196.e1-5. Epub 2011 Jul 27.
4. Williams JJ, Chawla N. Fractography of a neck failure in a double-modular hip implant. Case Stud Eng Fail Anal. 2014 Apr;2(1):45-50.
5. Mencière ML, Amouyel T, Taviaux J, Bayle M, Laterza C, Mertl P. Fracture of the cobalt-chromium modular femoral neck component in total hip arthroplasty. Orthop Traumatol Surg Res. 2014 Sep;100(5):565-8. Epub 2014 Aug 4.
6. Meftah M, Haleem AM, Burn MB, Smith KM, Incavo SJ. Early corrosion-related failure of the Rejuvenate modular total hip replacement. J Bone Joint Surg Am. 2014 Mar 19;96(6):481-7.
7. Kop AM, Swarts E. Corrosion of a hip stem with a modular neck taper junction: a retrieval study of 16 cases. J Arthroplasty. 2009 Oct;24(7):1019-23. Epub 2008 Oct 5.
8. Gill IP, Webb J, Sloan K, Beaver RJ. Corrosion at the neck-stem junction as a cause of metal ion release and pseudotumour formation. J Bone Joint Surg Br. 2012 Jul;94(7):895-900.
9. Kop AM, Keogh C, Swarts E. Proximal component modularity in THA—at what cost? An implant retrieval study. Clin Orthop Relat Res. 2012 Jul;470(7):1885-94.
10. Cooper HJ, Della Valle CJ, Berger RA, Tetreault M, Paprosky WG, Sporer SM, Jacobs JJ. Corrosion at the head-neck taper as a cause for adverse local tissue reactions after total hip arthroplasty. J Bone Joint Surg Am. 2012 Sep 19;94(18):1655-61.
11. Cooper HJ, Urban RM, Wixson RL, Meneghini RM, Jacobs JJ. Adverse local tissue reaction arising from corrosion at the femoral neck-body junction in a dual-taper stem with a cobalt-chromium modular neck. J Bone Joint Surg Am. 2013 May 15;95(10):865-72.
12. Restrepo C, Ross D, Restrepo S, Heller S, Goyal N, Moore R, Hozack WJ. Adverse clinical outcomes in a primary modular neck/stem system. J Arthroplasty. 2014 Sep;29(9)(Suppl):173-8. Epub 2014 May 27.
13. Lanting BA, Teeter MG, Vasarhelyi EM, Ivanov TG, Howard JL, Naudie DD. Correlation of corrosion and biomechanics in the retrieval of a single modular neck total hip arthroplasty design: modular neck total hip arthroplasty system. J Arthroplasty. 2015 Jan;30(1):135-40. Epub 2014 Jun 19.
14. De Martino I, Assini JB, Elpers ME, Wright TM, Westrich GH. Corrosion and fretting of a modular hip system: a retrieval analysis of 60 Rejuvenate stems. J Arthroplasty. 2015 Aug;30(8):1470-5. Epub 2015 Mar 14.
15. Gilbert JL, Buckley CA, Jacobs JJ. In vivo corrosion of modular hip prosthesis components in mixed and similar metal combinations. The effect of crevice, stress, motion, and alloy coupling. J Biomed Mater Res. 1993 Dec;27(12):1533-44.
16. Kwon YM. Evaluation of the painful dual taper modular neck stem total hip arthroplasty: do they all require revision? J Arthroplasty. 2016 Jul;31(7):1385-9. Epub 2016 Mar 21.
17. Gkagkalis G, Mettraux P, Omoumi P, Mischler S, Rüdiger HA. Adverse tissue reaction to corrosion at the neck-stem junction after modular primary total hip arthroplasty. Orthop Traumatol Surg Res. 2015 Feb;101(1):123-6. Epub 2015 Jan 22.
18. Molloy DO, Munir S, Jack CM, Cross MB, Walter WL, Walter WK Sr. Fretting and corrosion in modular-neck total hip arthroplasty femoral stems. J Bone Joint Surg Am. 2014 Mar 19;96(6):488-93.
19. Burge AJ, Gold SL, Lurie B, Nawabi DH, Fields KG, Koff MF, Westrich G, Potter HG. MR imaging of adverse local tissue reactions around Rejuvenate modular dual-taper stems. Radiology. 2015 Oct;277(1):142-50. Epub 2015 Jun 1.
20. Walsh CP, Hubbard JC, Nessler JP, Markel DC. MRI findings associated with recalled modular femoral neck Rejuvenate and ABG implants. J Arthroplasty. 2015 Nov;30(11):2021-6. Epub 2015 May 19.
21. Fraitzl CR, Moya LE, Castellani L, Wright TM, Buly RL. Corrosion at the stem-sleeve interface of a modular titanium alloy femoral component as a reason for impaired disengagement. J Arthroplasty. 2011 Jan;26(1):113-9: 119.e1. Epub 2010 Jan 22.
22. Sporer SM, DellaValle C, Jacobs J, Wimmer M. A case of disassociation of a modular femoral neck trunion after total hip arthroplasty. J Arthroplasty. 2006 Sep;21(6):918-21.
23. Kouzelis A, Georgiou CS, Megas P. Dissociation of modular total hip arthroplasty at the neck-stem interface without dislocation. J Orthop Traumatol. 2012 Dec;13(4):221-4. Epub 2011 Dec 8.
24. Nawabi DH, Do HT, Ruel A, Lurie B, Elpers ME, Wright T, Potter HG, Westrich GH. Comprehensive analysis of a recalled modular total hip system and recommendations for management. J Bone Joint Surg Am. 2016 Jan 6;98(1):40-7.
25. Buente D, Huber G, Bishop N, Morlock M. Quantification of material loss from the neck piece taper junctions of a bimodular primary hip prosthesis. A retrieval study from 27 failed Rejuvenate bimodular hip arthroplasties. Bone Joint J. 2015 Oct;97-B(10):1350-7.
26. Buente D, Bryant M, Ward M, Neville A, Morlock M, Huber G. The taper corrosion pattern observed for one bi-modular stem design is related to geometry-determined taper mechanics. Med Eng Phys. 2017 Aug;46:79-88. Epub 2017 Jun 21.
27. Bryant M, Buente D, Oladokun A, Ward M, Huber G, Morlock M, Neville A. Surface and subsurface changes as a result of tribocorrosion at the stem-neck interface of bi-modular prosthesis. Biotribology. 2017 Jun;10:1-16.
28. Goldberg JR, Gilbert JL, Jacobs JJ, Bauer TW, Paprosky W, Leurgans S. A multicenter retrieval study of the taper interfaces of modular hip prostheses. Clin Orthop Relat Res. 2002 Aug;401:149-61.
29. Matthies AK, Racasan R, Bills P, Blunt L, Cro S, Panagiotidou A, Blunn G, Skinner J, Hart AJ. Material loss at the taper junction of retrieved large head metal-on-metal total hip replacements. J Orthop Res. 2013 Nov;31(11):1677-85. Epub 2013 Aug 5.
30. Di Laura A, Hothi H, Henckel J, Swiatkowska I, Liow MHL, Kwon YM, Skinner JA, Hart AJ. Retrieval analysis of metal and ceramic femoral heads on a single CoCr stem design. Bone Joint Res. 2017 May;6(5):345-50.
31. Bryant M, Farrar, R., Brummitt, K., Freeman, R, Neville A. Fretting corrosion of fully cemented polished collarless tapered stems: the influence of PMMA bone cement. Wear. 2013 Apr-May;301(1-2):290-9.
32. Langton DJ, Jameson SS, Joyce TJ, Gandhi JN, Sidaginamale R, Mereddy P, Lord J, Nargol AV. Accelerating failure rate of the ASR total hip replacement. J Bone Joint Surg Br. 2011 Aug;93(8):1011-6.
33. Hothi HS, Berber R, Whittaker RK, Blunn GW, Skinner JA, Hart AJ. The relationship between cobalt/chromium ratios and the high prevalence of head-stem junction corrosion in metal-on-metal total hip arthroplasty. J Arthroplasty. 2016 May;31(5):1123-7. Epub 2015 Nov 26.
34. Kwon YM, Lombardi AV, Jacobs JJ, Fehring TK, Lewis CG, Cabanela ME. Risk stratification algorithm for management of patients with metal-on-metal hip arthroplasty: consensus statement of the American Association of Hip and Knee Surgeons, the American Academy of Orthopaedic Surgeons, and the Hip Society. J Bone Joint Surg Am. 2014 Jan 1;96(1):e4.
35. Hothi HS, Kendoff D, Lausmann C, Henckel J, Gehrke T, Skinner J, Hart A. Clinically insignificant trunnionosis in large-diameter metal-on-polyethylene total hip arthroplasty. Bone Joint Res. 2017 Jan;6(1):52-6.

36. Werner SD, Bono JV, Nandi S, Ward DM, Talmo CT. Adverse tissue reactions in modular exchangeable neck implants: a report of two cases. J Arthroplasty. 2013 Mar;28(3):543.e13-5. Epub 2012 Nov 8.

37. Barlow BT, Assini J, Boles J, Lee YY, Westrich GH. Short-term metal ion trends following removal of recalled modular neck femoral stems. J Arthroplasty. 2015 Jul; 30(7):1191-6. Epub 2015 Feb 28.

38. Walsh CP, Hubbard JC, Nessler JP, Markel DC. Revision of recalled modular neck Rejuvenate and ABG femoral implants. J Arthroplasty. 2015 May;30(5):822-6. Epub 2014 Dec 5.

39. Dimitriou D, Liow MHL, Tsai TY, Leone WA, Li G, Kwon YM. Early outcomes of revision surgery for taper corrosion of dual taper total hip arthroplasty in 187 patients. J Arthroplasty. 2016 Jul;31(7):1549-54. Epub 2016 Jan 21.

40. Liow MHL, Urish KL, Preffer FI, Nielson GP, Kwon YM. Metal ion levels are not correlated with histopathology of adverse local tissue reactions in taper corrosion of total hip arthroplasty. J Arthroplasty. 2016 Aug;31(8):1797-802. Epub 2016 Feb 4.

41. Walker P, Campbell D, Della Torre P, Brazil D, McTighe T. Trunnion corrosion and early failure in monolithic metal-on-polyethylene TMZF femoral components: a case series. Reconstructive Review. 2016 Sep;6(3):13-8.

42. Matsen Ko L, Chen AF, Deirmengian GK, Hozack WJ, Sharkey PF. Catastrophic femoral head-stem trunnion dissociation secondary to corrosion. J Bone Joint Surg Am. 2016 Aug 17;98(16):1400-4.

43. Banerjee S, Cherian JJ, Bono JV, Kurtz SM, Geesink R, Meneghini RM, Delanois RE, Mont MA. Gross trunnion failure after primary total hip arthroplasty. J Arthroplasty. 2015 Apr;30(4):641-8. Epub 2014 Nov 26.

44. Cleary PD, Reilly DT, Greenfield S, Mulley AG, Wexler L, Frankel F, McNeil BJ. Using patient reports to assess health-related quality of life after total hip replacement. Qual Life Res. 1993 Feb;2(1):3-11.

45. Schurman DJ, Bloch DA, Segal MR, Tanner CM. Conventional cemented total hip arthroplasty. Assessment of clinical factors associated with revision for mechanical failure. Clin Orthop Relat Res. 1989 Mar;240:173-80.

46. Krull A, Morlock MM, Bishop NE. The influence of contamination and cleaning on the strength of modular head taper fixation in total hip arthroplasty. J Arthroplasty. 2017 Oct;32(10):3200-5. Epub 2017 May 13.

47. Haschke H, Jauch-Matt SY, Sellenschloh K, Huber G, Morlock MM. Assembly force and taper angle difference influence the relative motion at the stem-neck interface of bi-modular hip prostheses. Proc Inst Mech Eng H. 2016 Jul;230(7): 690-9. Epub 2016 May 10.